Selection of High-Affinity RNA Ligands to Reverse Transcriptase: Inhibition of cDNA Synthesis and RNase H Activity†

Hang Chen and Larry Gold*

Department of Molecular, Cellular, and Developmental Biology, University of Colorado, Boulder, Colorado 80309

Received December 13, 1993; Revised Manuscript Received May 16, 1994®

ABSTRACT: Specific, high-affinity RNA ligands to avian myeloblastosis virus and Moloney murine leukemia virus reverse transcriptases were isolated from a combinatorial RNA library using the SELEX (*s*ystematic *e*volution of *l*igands by *ex*ponential enrichment) procedure. The selected RNA ligands bound their respective reverse transcriptases with approximately nanomolar dissociation constants. The ligands did not exhibit primary sequence conservation from selections against different target enzymes. Moreover, the selected ligands competed with the binding of template/primer complex and inhibited both the RNA-dependent DNA polymerase and the RNase H activities of the cognate reverse transcriptase. SELEX can yield both high-affinity and high-specificity oligonucleotide antagonists against specific members of a protein family.

Retroviruses contain diploid RNA genomes that are replicated through a DNA intermediate by reverse transcriptase (RT)[1] (Baltimore, 1970; Temin & Mizutani, 1970; Weiss et al., 1982, 1985). The retroviral genome typically consists of three open reading frames: *gag*, *pol*, and *env*. RT is encoded by the *pol* gene, and the primary structure of retroviral RTs is conserved. The maturation of RT usually requires posttranslational processing by proteolysis. The multifunctional RT has both RNA-dependent and DNA-dependent DNA polymerization activities, as well as RNase H activity. RNase H hydrolyzes the RNA strand of the RNA–DNA hybrid to create the primer for the second strand DNA synthesis (Varmus, 1987; Goff, 1990; Jacobo-Molina & Arnold, 1991). The polymerization domain of RT is located at the N-terminus, while the RNase H domain is located at the C-terminus (Jacobo-Molina & Arnold, 1991). The two domains are separated by a distance of about 50 Å and can be filled by 16–18 base pairs of A-form helix (Johnson et al., 1986; Oyama et al., 1989; Furfine & Reardon, 1989; Kohlstaedt et al., 1992).

Avian myeloblastosis virus (AMV) RT is a heterodimer of 63 and 95-kDa subunits (Varmus & Swanstrom, 1984). AMV RT preferentially interacts with $tRNA^{Trp}$ of the host for priming cDNA synthesis (Bishop, 1978; Garret et al., 1985). Moloney murine leukemia virus (M-MLV) RT is an 80-kDa monomer (Varmus & Swanstrom, 1984) that prefers $tRNA^{Pro}$ over other species for priming cDNA synthesis, but has less specificity for tRNA molecules from the host (Jacobo-Molina & Arnold, 1991). RT is packaged in the retroviral particles (Vaishnav & Wong-Staal, 1991). After the virus enters the host cell, the genomic RNA molecules, RT, integrase, nuclear capsid protein, and other encapsidated molecules are released. RNA is reverse transcribed into double-stranded DNA by RT, and this proviral DNA is integrated into the host genome for its expression (Vaishnav & Wong-Staal, 1991). RT is one preferred target for anti-retroviral therapy: inhibition of RT activity may block the retroviral life cycle at an early stage.

In the present work we employed the SELEX (*s*ystematic *e*volution of *l*igands by *ex*ponential enrichment) procedure (Tuerk & Gold, 1990) to isolate inhibitory, high-affinity RNA ligands from a randomized RNA molecular repertoire against AMV and M-MLV RT, respectively. Oligonucleotides can form intricate structures presenting potentially optimized binding surfaces, and thus it is possible to select high-affinity single-stranded oligonucleotides against nearly any desired target (Gold et al., 1993). In practice, SELEX yields nucleic acid molecules with high-affinity for the target, and the selected ligand usually has higher affinity than that of any natural nucleic acid ligand (Schneider et al., 1992; Gold et al., 1993). SELEX has provided high-affinity ligands for several target molecules, including nucleic acid binding proteins (Tuerk & Gold, 1990; Bartel et al., 1991; Schneider et al., 1992; Tuerk et al., 1992, 1993), non-nucleic acid binding proteins (Bock et al., 1992; J. Binkley et al., manuscript in preparation; Jellinek et al., 1993; Kubik et al., 1993), organic dyes (Ellington & Szostak, 1990, 1992), and small molecules (Connell et al., 1993; Sassanfar & Szostak, 1993; Jenison et al., 1994). We have found that high-affinity RNA ligands isolated against AMV RT or M-MLV RT can severely inhibit polymerization and RNase H activities of reverse transcriptase. Our results address the value of SELEX in identifying inhibitory ligands that discriminate between proteins from within a conserved protein family.

EXPERIMENTAL PROCEDURES

Materials. AMV reverse transcriptase was purchased from Life Sciences, Inc.; M-MLV reverse transcriptase, from GIBCO BRL; Taq DNA polymerase, from Promega; T4 polynucleotide kinase, from New England Biolabs; RNase T1, from Boehringer Mannheim; and T7 RNA polymerase, from United States Biochemical Corporation. The chemical reagent dimethyl sulfate (DMS) was obtained from Aldrich Chemical Company; 2-oxo-3-ethoxybutyraldehyde (kethoxal), from United States Biochemical Corporation; and 1-cyclohexyl- 3-(2-morpholinoethyl)carbodiimide metho-*p*-toluenesulfonate (CMCT), from Sigma Chemical Corporation.

† This work was funded by research grants from the National Institutes of Health to L.G. (GM-28685 and GM-19963) and funds from NeXagen, Inc., Boulder, CO.

* Corresponding author.

® Abstract published in *Advance ACS Abstracts,* July 1, 1994.

[1] Abbreviations: AMV, avian myeloblastosis virus; CMCT, 1-cyclohexyl-3-(2-morpholinoethyl)carbodiimide metho-*p*-toluenesulfonate; DMS, dimethyl sulfate; DTT, dithiothreitol; Kethoxal, 2-oxo-3-ethoxybutyraldehyde; M-MLV, Moloney murine leukemia virus; RT, reverse transcriptase; SELEX, *s*ystematic *e*volution of *l*igands by *ex*ponential enrichment.

0006-2960/94/0433-8746$04.50/0

Table 1: Oligonucleotides Used in the Experiments

name	sequence
DNA [a]	
CH1	5'-CCCGGATCCTAGTTCACGATGCTGCAA-N12-GCGC-N12-GCGC-N12 TTACGGTCTGAGAAAATATCCTCC-3'
CH2	5'-CCCAAGCTTAATACGACTCACTATAGGGAGGATATTTTCTCAGACCGTAA-3'
CH3	5'-CCCGGATCCTAGTTCACGATGCTGCAA-3'
I-3	5'-CCCACGTCACGACGTTGTAAAACGACGCCC-3'
H-2	5'-CTTACTTTTGTTTTGCTCTTCCTCTATCTTGTCTAAAGC-3'
RNA [b]	
H-1	5'-GGGAAUUCGAGCUCAAGCUUUAGACAAGAUAGAGGAAGAGCAAAACAAAAG UAAGAAAAAAGCACAGCAAGCAGCAGCUGGGAUC-3'
da.1.1	5'-CGUCCCGUGCGCAAAAGUUCUUAGCGCUAGCAGUCCUAGuugc-3'
dm.1.1	5'-UUACCACGCGCUCUUAACUGCUAGCGCCAUGGC-3'
F-1 [c]	5'-GGGAAUUCGAGCUCGGUACCCGGGAUCCUCUAGAGUCGACCUGCAGGCAU GCUAGCUUGGCACUGGGCGUCGUUUUACAACGUCGUGACGUGGG-3'

[a] DNA oligonucleotide CH1 is the template for the starting RNA pool. Oligonucleotides CH2 and CH3 are the 5′ and 3′ PCR primers, respectively. CH2 contains a T7 promoter, and CH3 was also used for priming cDNA synthesis during SELEX and sequencing. Oligonucleotide I-3 was used as a primer to form the template/primer complex in the inhibition of polymerization and competitive binding assays. H-2 is a fragment of DNA used in the RNase H activity assay to form an RNA–DNA hybrid with H-1 (Mizrahi, 1989). [b] RNA oligonucleotide H-1 is derived from the HIV-1 genome and was used to form an RNA–DNA hybrid with H-2 in the RNase H activity assay (Mizrahi, 1989). RNA oligonucleotides da. 1.1 and dm. 1.1 are the minimum sequences of a.1.1 and m.1.1, respectively. The lowercase letters represent the sequences in the fixed region. [c] F-1 is an RNA fragment transcribed in vitro from plasmid pT7-1 and was used as an RNA template to form the template/primer complex for the polymerization inhibition assay as well as the competitive binding assay (Craig et al., 1993).

Table 2: Summary of the SELEX Procedure

	AMV reverse transcriptase				M-MLV reverse transcriptase			
round	input RNA (nM)	protein[a] (nM)	apparent[b] K_d (nM)	background[c] (%)	input RNA (nM)	protein[a] (nM)	apparent[b] K_d (nM)	background[c] (%)
starting pool	200	32		0.50	200	64		0.50
1st round	200	32	379	0.40	200	64		0.56
3rd round	200	16	195	1.40	200	64		0.90
6th round	150	7	14	2.06	150	32	150	0.90
9th round	150	2.8	5.7	2.20	150	27	54	0.80
12th round	100	0.8	1.4	2.50	100	16	36	1.30
15th round					100	6	12	2.00
17th round					50	4	7.6	2.20

[a] Protein concentration was decreased every three rounds in order to retain high stringency. [b] The apparent dissociation constant of the RNA pool for the cognate RT. [c] The background is the percentage of RNA bound to a nitrocellulose filter in the absence of protein.

Radioactive nucleotides [α-^{32}P] GTP and [γ-^{32}P] ATP were purchased from New England Nuclear, Inc. DNA and RNA oligonucleotides (Table 1) were synthesized on an Applied Biosystems Model 394 DNA/RNA synthesizer.

Nucleic Acids. RNAs were synthesized by *in vitro* transcription of PCR-amplified DNA oligonucleotides. PCR amplification was performed in 50 mM KCl, 10 mM Tris-HCl, pH 8.6, 2.5 mM $MgCl_2$, 170 μg/mL BSA, 1 mM dNTPs, 5 units per 100 μL Taq DNA polymerase, and 1 μM 5′ and 3′ primers. The transcription reaction was conducted in 40 mM Tris-HCl, pH 8.0, 12 mM $MgCl_2$, 5 mM DTT, 1 mM spermidine, 0.002% Triton X-100, 8% PEG 8000, 2 mM NTPs, and 1 unit/μL T7 RNA polymerase at 37 °C for 2 h followed by addition of 20 units of DNase I and incubation at 37 °C for 5 min. The transcribed RNA was purified on a 10% polyacrylamide/8 M urea gel. Synthesis of internally ^{32}P-labeled RNA was performed as above except the reaction buffer contained 0.5 mM ATP, CTP, and UTP, along with 0.05 mM GTP and 0.33 mM [α-^{32}P] GTP (800 Ci/mmol).

Selection Procedure. High-affinity RNA ligands were selected from a starting RNA repertoire containing 10^{14} unique species as described previously (Tuerk & Gold, 1990; Tuerk et al., 1992). Selection was performed in 1 mL of binding buffer (50 mM Tris-HCl, pH 7.7, 200 mM potassium acetate, and 10 mM DTT) containing RNA and target protein as indicated in Table 2. The binding reaction was incubated at 37 °C for 5 min, and bound RNA was partitioned by nitrocellulose filtration. The bound RNA was eluted into 200 μL of 7 M urea and 400 μL of phenol as described by Tuerk and Gold (1990), recovered by ethanol precipitation, and used to generate cDNA. The cDNA product was amplified by PCR and transcribed with T7 RNA polymerase (Tuerk & Gold, 1990) to generate the RNA pool for the next round of selection. Importantly, cDNA from the AMV RT selection was synthesized by M-MLV RT, while cDNA from

Table 3: RNA Sequences from AMV RT Selection[a]

Starting Pool

5'-gggaggauauuuucucagaccguaa-N12-gcgc-N12-gcgc-N12-uugcagcaucgugaacuaggauccggg-3'

	Kd(nM)	Freq.	Name	Structure
AGGUCGUCCCGU gcgc AAAAGUUCUUA gcgc UAGCAGUCCUAGuugc	0.5	13/57	a.1.1	dual hairpin
UUCCUGUCCUCG gcgc UUCGCUUUAAU gcgc GCUGGUAAGUUG	1.6	7/57	a.1.2	pseudoknot
CCUGAUACUGAU gcgc UUCCGUGCUCU gcgc GUUGAUUAAUG	2.0	6/57	a.1.3	stem-loop w/bulge
CUUCUUGCUACG gcuc CGUGCGUCUC gcgc UUUAAACCCUG	2.4	9/57	a.1.4	stem-loop w/bulge
UCGUUGGACUUG gcgc UCCCACACAAA gcgc GCUACCUAGCUCC	2.8	7/57	a.1.5	pseudoknot
CCGUUCUAAGAU gcgu CUCCAUCUAUCC ggca UUAGCUUCGGUU	6.1	8/57	a.1.6	pseudoknot
UCGUUCACUUC gcac UAAAAAAUGUAUG gcgc AGUAGCUCGCUG	7.3	7/57	a.1.7	pseudoknot

[a] The sequences are obtained by cloning and sequencing after 12 rounds of selection by AMV RT. cDNA of the round 12 RNA repertoire was cloned into pUC18 vector by *Bam*HI and *Hin*dIII digestion. The apparent K_d's, the frequencies of the sequences, and the names and possible secondary structures are shown. The uppercase letters indicate the variable regions, the lowercase ones indicate the fixed regions, and the underlined letters represent the mutations in the fixed regions. The possible secondary structures were obtained by a computer RNA folding algorithm (Zuker, 1989; Jaeger et al., 1989). The arrows indicate the base pairs.

the M-MLV RT selection was synthesized by AMV RT, at 45 °C.

Determination of Equilibrium Dissociation Constants. Equilibrium dissociation constants were measured as described by Corey et al. (1983). The binding reaction contained 7×10^{-11} M internally ^{32}P-labeled RNA and 7×10^{-11} to 2×10^{-7} M protein in 60 μL of binding buffer. The reaction mixture was incubated at 37 °C for 5 min, and 30 μL of the binding reaction mixture was filtered through nitrocellulose. Filters were dried and assayed by scintillation counting with Ecolume (ICN, Inc.) in a Beckman LS-133 scintillation counter. Equilibrium dissociation constants were determined by plotting the percentage of RNA bound versus the log protein concentration (Klotz, 1985).

Boundary Analysis. Determination of the 5′ and 3′ boundaries required for protein binding was performed as described by Tuerk et al. (1990). Briefly, RNA was partially hydrolyzed by incubation in 50 μL of 50 mM sodium carbonate, pH 9.0, 1 mM EDTA, and 0.5 mg/mL yeast tRNA at 90 °C for 15 min. The reaction was neutralized by addition of 6 μL of 3 M sodium acetate pH 5.2, followed by ethanol precipitation. The 3′ boundary was determined by incubating 30 pmol of partially alkaline hydrolyzed ^{32}P 5′-end-labeled RNA with protein in 1 mL of binding buffer as described previously (Tuerk et al., 1990). Likewise, the 5′ boundary was determined by incubating partially alkaline hydrolyzed unlabeled RNA with protein followed by primer extension with ^{32}P 5′-end-labeled oligonucleotide CH3 as indicated above.

Chemical Modification. Chemical modification was performed as described by Stern et al. (1988). RNA was incubated in binding buffer at 90 °C for 3 min and rapidly cooled on ice for 15 min. One picomole of RNA in 50 μL was incubated in the presence of 5 μL of chemical reagent (DMS, 1/60 dilution in ethanol; kethoxal, 12.5 μg/μL; CMCT, 30 μg/μL in buffer) at 37 °C for 8 min. The protein footprint was obtained under the same conditions with the exception that 1 pmol of RNA was preincubated with 4 pmol of protein at 37 °C for 5 min prior to addition of the modification reagents. RNAs were analyzed by primer extension of ^{32}P 5′-end-labeled oligonucleotide CH3 to determine the position of the modified nucleotide (Stern et al., 1988; Barta et al., 1984; Shelness & Williams, 1985).

Inhibition of RT Polymerization Activity. The polymerization inhibition assay was performed as described by Tuerk et al. (1992). The reaction mixture contained 3.2 nM RT, 10 nM template/^{32}P 5′-end-labeled primer complex, and RNA ligand as indicated in Results. The inhibition assay was performed at 37 °C for 10 min in 20 μL of polymerization buffer (50 mM Tris-HCl, pH 7.7, 200 mM potassium acetate, 6 mM $MgCl_2$, 10 mM DTT, and 0.4 mM dNTPs). The polymerization products were analyzed by electrophoresis on a 7 M urea/10% polyacrylamide gel.

Competitive Binding Assay. Template/primer complex was formed by annealing 200 pmol of F-1 RNA with 200 pmol of oligonucleotide I-3′ in 50 μL of annealing buffer (50 mM Tris-HCl, pH 7.7, and 200 mM potassium acetate). The annealing reaction mixture was incubated at 65 °C for 5 min, slowly cooled to room temperature for 1 h, and stored on ice. An equimolar ratio of RT and template/^{32}P 5′-end-labeled primer complex was incubated with unlabeled RNA ligand in 60 μL of binding buffer at 37 °C for 5 min. The binding of template/primer complex was analyzed by nitrocellulose filtration as described previously (Tuerk et al., 1990, 1992). The binding of the template/primer complex to each RT was not 100% at the concentrations used. Therefore, all data were normalized to the percentage of template/primer complex bound in the absence of a competing ligand.

Inhibition of RNase H Activity. Briefly, the RNA–DNA hybrids were formed as described by Mizrahi (1989). Ten picomoles of ^{32}P 5′-end-labeled RNA H-1 and 100 pmol of DNA oligonucleotide H-2 were incubated in 50 μL of 40 mM Tris-HCl, pH 7.7, 40 mM KCl, and 4 mM $MgCl_2$ at 65 °C for 5 min, slowly cooled to room temperature for 1 h, and stored on ice. Inhibition of the RNase H activity was assayed by incubating 12.5 nM RNA–DNA hybrid with RT and RNA ligand. The reaction was performed in 10 μL of buffer (50 mM Tris-HCl, pH 7.7, 50 mM KCl, 7 mM $MgCl_2$, and 5 mM DTT), and the mixture was incubated at 37 °C for 5 min. The reaction was stopped by adding 1 μL of 0.5 M EDTA, pH 8.0.

RESULTS

High-Affinity RNA Ligands Against AMV RT. High-affinity RNA ligands against AMV RT were selected from a starting RNA repertoire consisting of three 12-nucleotide

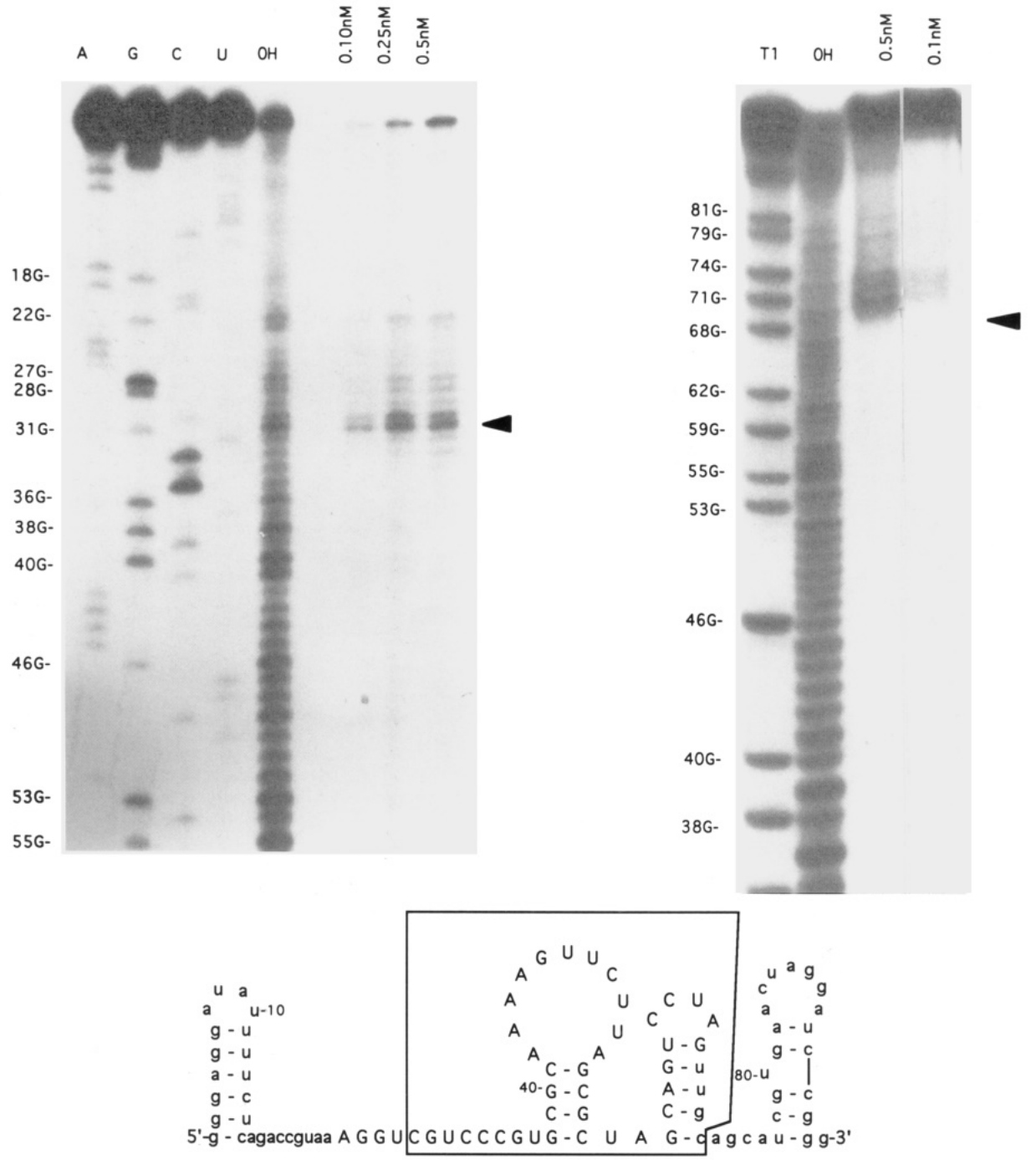

FIGURE 1: AMV RT binding boundary of ligand a.1.1. (A, top left) 5′ boundary of ligand a.1.1. A, G, C, U, and OH lanes: RNA sequencing and alkaline partial hydrolysis. The right three lanes show the boundary with varying amounts of AMV RT as indicated. The arrowhead indicates the boundary position. (B, top right) 3′ boundary of ligand a.1.1. T1, RNase T1 partial digestion; OH, alkaline partial hydrolysis; AMV RT concentration, as indicated. The arrowhead indicates the boundary position. (C, bottom) Summary of the AMV RT binding boundary of ligand a.1.1. The box indicates the minimum binding sequence. Lowercase letters represent the fixed sequences.

randomized regions separated by two GCGC fixed sequences and flanked by primer binding sequences (25 nucleotides at the 5′-end and 27 nucleotides at the 3′-end) (Tables 1 and 3). The complexity of the starting RNA repertoire approached 10^{14} species. The selection conditions are summarized in Table 2. The cDNA was synthesized with M-MLV RT. The binding affinity of the starting pool was in the micromolar range. After 12 rounds of selection, the affinity of the RNA pool increased about 10^3-fold over the original randomized pool (Table 2). The repertoire was analyzed by sequencing of the bulk RNA of round 12 selection (not shown). It showed that the complexity of the RNA repertoire was reduced and the affinity increased.

Fifty-seven reliable RNA sequences were obtained by cloning and sequencing of the cDNA from the round 12 selection pool (Table 3). It was noticed that point mutations and deletions were introduced into some RNA molecules. Interestingly, all of the sequences showed some duplicates without orphan species. The dissociation constants of the individual RNA species were measured between 0.5 and 7.3 nM. The RNA ligands from the AMV RT SELEX can be classified into three groups on the basis of the similarities of sequences and possible secondary structures (Table 3). The highest affinity RNA ligand (designated ligand a.1.1) forms a dual hairpin structure. Ligands a.1.2, a.1.5, a.1.6, and a.1.7 may form pseudoknots. Ligands a.1.3 and a.1.4 form stem-

loops with internal bulge structures containing a GUCU consensus sequence in the central loop. Because RNA ligand a.1.1 has the highest binding affinity, it was chosen for further studies.

Boundary Determinations and Footprint Analysis of Ligand a.1.1. The highest affinity RNA ligand selected by AMV RT (ligand a.1.1) was further analyzed to determine the minimum sequence required for specific interaction with its target protein. The minimum domain contains 43 nucleotides (from C30 to G72) (Figure 1). The 5′ hairpin results from hybridization of the two GCGC fixed sequences, leaving 11 nucleotides in the loop. The 3′ hairpin is formed by a portion of the 3′ variable region and the 3′ fixed sequence. A one-nucleotide deletion occurred within the first loop.

The validity of this RNA structure interaction with AMV RT was investigated by protein binding protection (footprint) studies. The chemical probing and footprint data derived from treatment of the RNA and the RNA–protein complex with the structure-specific chemical reagents DMS (modifies A and weakly modifies C), kethoxal (modifies G), and CMCT (modifies U) followed by primer extension (Stern et al., 1988) were consistent with the predicted secondary structure and boundary results. Most of the nucleotides in the single-strand region within the boundary were protected completely or to some extent in the presence of AMV RT. However, nucleotides A42, A43, U48, U51, and A52 in the 5′ loop, A58 in the connection of the two stem-loops, and U66 and A67 in the 3′ loop were accessible to the chemical reagents in solution in the presence as well as in the absence of AMV RT (Figure 2). These bases may protrude out of the RNA binding site of AMV RT into the solvent. Moreover, the 3′ stem-loop structure appears to form a weak secondary structure and is only weakly protected by AMV RT. The illustrated secondary structure for ligand a.1.1 was predicted using a computer RNA folding algorithm (Zuker, 1989; Jaeger et al., 1989).

A truncated RNA ligand (designated da.1.1; Table 1) was synthesized based on the AMV RT binding boundary study; da.1.1 bound to AMV RT with a K_d of 13.6 nM. The binding affinity for AMV RT was considerably lower than that observed with the intact ligand a.1.1 (K_d, 0.5 nM). The flanking sequences might either stabilize the RNA secondary structure or contribute to the binding by nonspecific interactions with AMV RT.

High-Affinity RNA Ligands against M-MLV RT. Selection was also performed using M-MLV RT as the target and the same starting RNA repertoire as in the previous section. Table 2 shows the summary of the selection conditions. In order to isolate the RNA ligands that are not only tight binders but also inhibitors for M-MLV RT, AMV RT was used to make cDNA from RNA selected by M-MLV RT. The starting RNA repertoire had lower affinity for M-MLV RT with a K_d greater than 1 μM. After 17 rounds of selection with M-MLV RT, the binding affinity of the RNA pool was increased 10^3-fold over that of the starting RNA repertoire (Table 2), and the complexity of the round 17 selection pool was decreased (data not shown).

The round 17 RNA pool was analyzed by cDNA cloning and sequencing (Table 4). No obvious sequence similarities in the RNA molecules were found between the AMV RT and M-MLV RT SELEX experiments. However, secondary structure similarities were observed, including the shared potential for adopting pseudoknot structures. The RNA ligands selected for binding to M-MLV RT belong to two major groups. The first group, which has the highest binding affinity to M-MLV RT, forms a stem-loop with an internal bulge structure. Members of the second group (m.1.2, m.1.3, m.1.4, and m.1.5) have the potential to form pseudoknot structures (Table 4). A consensus sequence of CCCRRYGAA (R represents purine, and Y represents pyrimidine) was found in the 5′ variable region, and a consensus sequence of

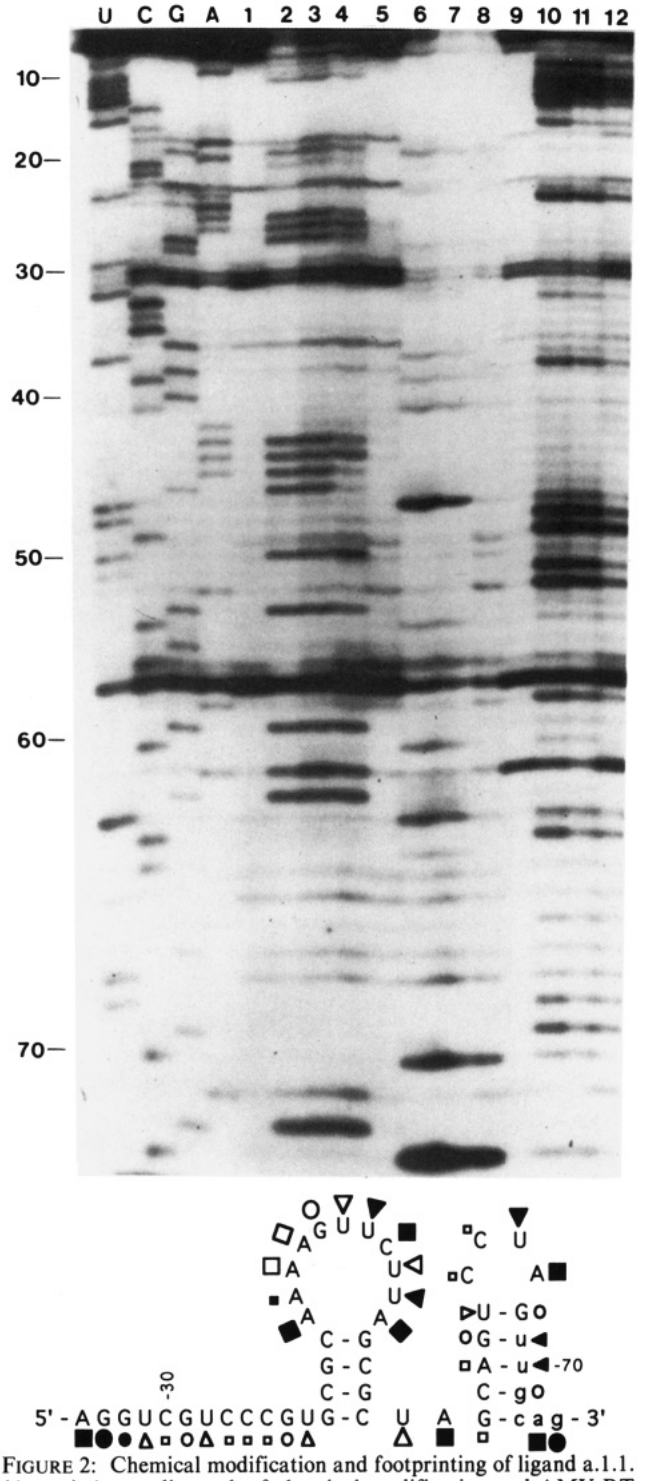

FIGURE 2: Chemical modification and footprinting of ligand a.1.1. (A, top) Autoradiograph of chemical modification and AMV RT binding protection of a.1.1. A, G, C, and U, RNA sequencing lanes; lanes 1, 5, and 9, control; lanes 2, 3, and 4, DMS modification; lane 4 in the presence of AMV RT; lanes 6, 7, and 8, kethoxal modification, lane 8 in the presence of AMV RT; lanes 10, 11, and 12, CMCT modification, lane 12 in the presence of AMV RT. Lanes 2, 6, and 10, the modification reactions were carried out immediately, while others were kept on ice for 15 min then carried out modification. The numbers indicate the nucleotide position in RNA ligand a.1.1. (B, bottom) Results of chemical modification. The size of each symbol represents the extent of modification: square, DMS modification; circle, KE modification; triangle: CMCT modification. An open symbol means protection of modification in the presence of protein; a filled symbol means modification in the presence of protein.

Table 4: RNA Sequences from M-MLV RT Selection[a]

Starting Pool

5'-gggaggauauuuucucagaccguaa-N12-gcgc-N12-gcgc-N12-uugcagcaucgugaacuaggauccggg-3'

	Kd(nM)	Freq.	Name	Structure
CUUACCAC gcgc UCUUAACUCGUA gcgc CAUGGCCAAAACU	6.9	9/45	m.1.1	stem-loop w/bulge
CAUCCCAGCGAA gg AUACCGCUGUG gcgc CCUCUUUCACAU	10.0	6/45	m.1.2	pseudoknot
UUCCCAGCGAAA gg AUACCGGCUGUG gcgc CCUCUUUCACAU	10.0	5/45	m.1.3	pseudoknot
AUCCCCGAUGAA gcgc GAUACCAUCGG gcgc GACUACCCCUG	12.5	12/45	m.1.4	pseudoknot
CCCACGUGAAUC gcgc AUACCUCGUGG ccgc AUCCUCCGAUACA	23.0	13/45	m.1.5	pseudoknot

[a] The sequences are obtained by cloning and sequencing after 17 rounds of selection by M-MLV RT. The other descriptions are the same as in Table 3.

$AUACCN_{2-4}GUGGC$ (N can be any of the four nucleotides) was found in the central randomized region of the second group.

Boundary Determination and Footprint Analysis of Ligand m.1.1. The highest affinity RNA ligand m.1.1 for M-MLV RT was further characterized to identify the minimum sequence required for specific interaction with M-MLV RT and to determine the secondary structure of RNA, as described in the previous section. The boundary results suggest that a stem-loop structure (from nucleotide position 27 to 59) with an internal bulge formed by the variable regions and the GCGC fixed sequences provides most of the binding interactions with M-MLV RT (Figure 3).

Footprint (Stern et al., 1988) data of ligand m.1.1 was consistent with the boundary determination results, with the exception that U40, U41, A43, U45, and U48 in the loop and A55 in the dinucleotide bulge were accessible to the chemical reagents in the presence as well as in the absence of M-MLV RT (Figure 4). To further confirm the proposed structure, a truncated RNA molecule (designated dm.1.1; Table 1) with the sequence of the minimum binding domain defined by the boundary experiments was synthesized and examined for the binding affinity to M-MLV RT. The affinity (K_d, 18.5 nM) for the truncated version of the RNA molecule was comparable to that observed with the intact ligand m.1.1 (K_d 6.9 nM). We also designed another truncated version of m.1.1 in which the 10-nucleotide loop was replaced with a UUCG tetraloop. The binding affinity of this RNA molecule to M-MLV RT was not detectable at all under our conditions (data not shown). The results suggested that the size and composition of the loop is crucial for interaction with M-MLV RT.

Inhibition of RT Polymerization Activity by Selected RNA Ligands. The ability of the selected RNA ligands to inhibit the RNA-dependent DNA polymerization activity of AMV RT and M-MLV RT was examined. A template/primer complex derived from a fragment of plasmid pT7-1 (Table 1) was used for primer extension (Tuerk et al., 1992) by AMV RT and M-MLV RT, respectively. The ligand a.1.1 inhibited AMV RT polymerization activity with an IC_{50} (50% inhibition of activity) approximately equal to 25 nM (Figure 5, panels A and E). In a similar assay, ligand a.1.1 inhibited M-MLV RT activity less effectively, with an IC_{50} about 120 nM (Figure 5B).

The ability of the RNA ligand m.1.1 to inhibit the RNA-dependent DNA polymerization activity of M-MLV RT was also studied. The RNA ligand m.1.1 severely inhibited M-MLV RT with an IC_{50} approximately equal to 9 nM (Figure 5, panels C and E), while it had very little effect on AMV RT (Figure 5D). Therefore, this RNA ligand inhibits M-MLV RT both efficiently and specifically. The starting RNA repertoire used to initiate the selection procedures did not inhibit the polymerization activities of either AMV RT or M-MLV RT, even up to 1 μM concentration (data not shown).

Competitive binding assays were performed to help decipher the mechanism of inhibition of AMV RT and M-MLV RT binding to the template/primer complex by selected ligands. An apparent dissociation constant (K_d) of the template/primer complex used in the inhibition experiments (Tuerk et al., 1992) (Table 1) was measured at about 12 nM for AMV RT and about 91 nM for M-MLV RT. If the selected RNA ligands interact with RT in the active site, the template/primer complex and the selected RNA ligands will compete with each other for binding to this site. The binding competition was performed by incubation of labeled template/primer junction and AMV RT at equimolar ratio (32 nM) with varying amounts of unlabeled selected RNA ligand (Figure 6). RNA ligand a.1.1 competes with template/primer complex for interaction with AMV RT. Similarly, a competitive binding assay of template/primer complex to M-MLV RT with RNA ligand m.1.1 was also performed (Figure 6). An equimolar ratio of M-MLV RT (90 nM) and template/primer complex (90 nM) was used. The binding of labeled template/primer complex to M-MLV RT can be competed by the ligand m.1.1.

In order to understand whether the selected RNA ligands can discriminate their targets, we also performed the nitrocellulose binding assays to test the binding affinities of the ligands to the cognate as well as the noncognate target protein. The AMV RT selected ligand a.1.1 bound to the noncognate M-MLV RT with a K_d of about 44 nM (Figure 7); thus the affinity of ligand a.1.1 to M-MLV RT was over 80-fold lower than that to the cognate target AMV RT (K_d, 0.5 nM). Similarly, the M-MLV RT selected RNA ligand m.1.1 interacted with the noncognate AMV RT with a dissociation constant in the micromolar range (Figure 7), while the K_d of ligand m.1.1 for its cognate M-MLV RT was 6.9 nM. The results indicated that the selected RNA ligands could discriminate the targets within a protein family. The inhibition ability of ligand a.1.1 to M-MLV RT could be interpreted that this ligand bound to the noncognate M-MLV RT with low affinity.

Inhibition of RT-Associated RNase H Activity by Selected RNA Ligands. The selected RNA ligands were examined for the ability to inhibit RT-associated RNase H activity. An RNA–DNA hybrid derived from the HIV-1 genome (Table

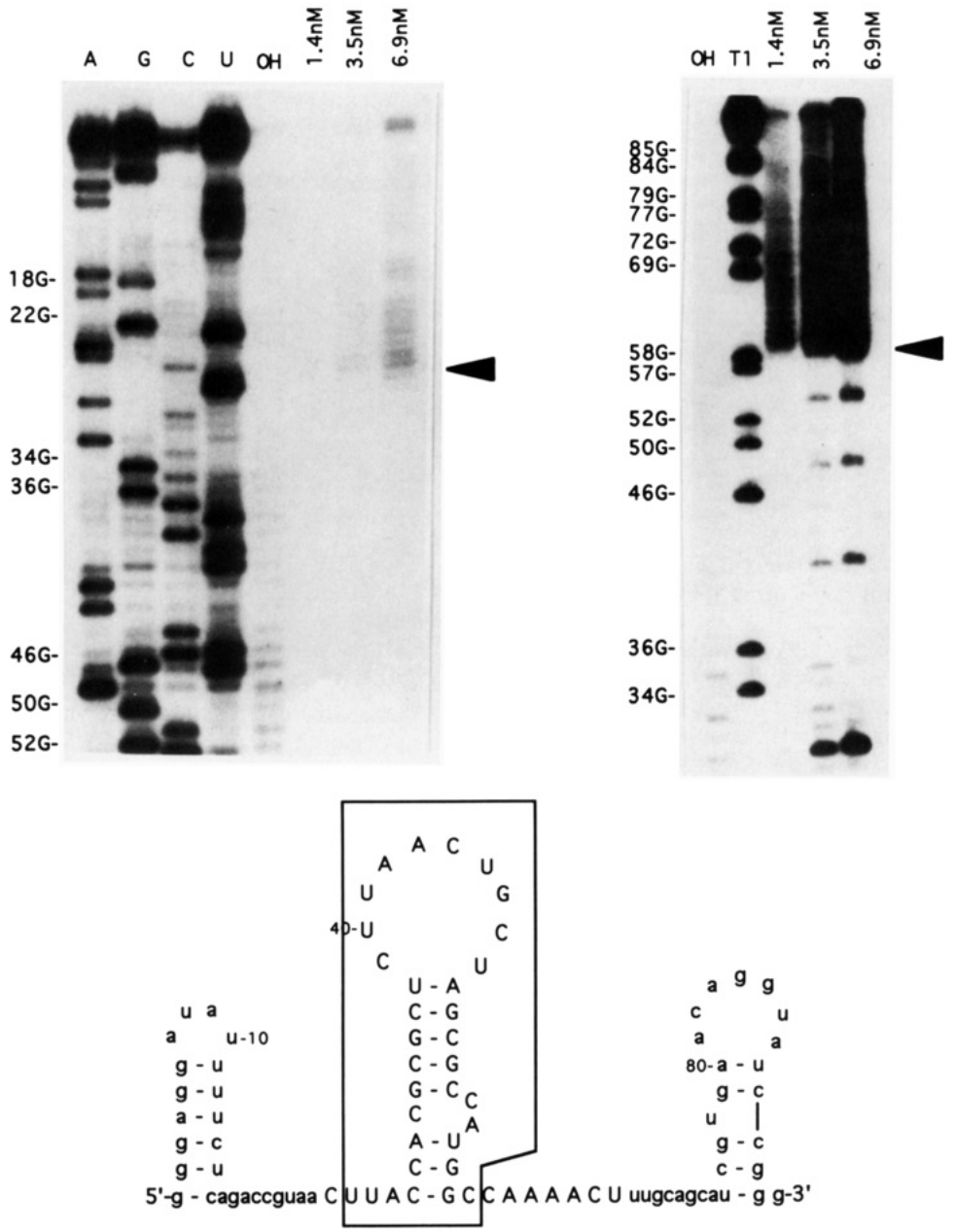

FIGURE 3: M-MLV RT binding boundary of ligand m.1.1. (A, top left) 5′ boundary of ligand m.1.1. A, G, C, U, and OH, RNA sequencing and alkaline partial hydrolysis. The right three lanes show the binding boundary with different M-MLV RT concentrations as indicated. The arrowhead indicates the boundary position. (B, top right) 3′ boundary of ligand m.1.1. OH, alkaline partial hydrolysis; T1, RNase T1 partial digestion. The right three lanes show the binding boundary with different M-MLV RT concentrations (as indicated). The arrowhead indicates the boundary position. (C, bottom) Summary of AMV RT binding boundary of ligand m.1.1. The box indicates the minimum binding sequence. Lowercase letters represent the fixed sequences.

1) was employed as the substrate for the RNase H cleavage experiment (Mizrah, 1989). The hybrid labeled with ^{32}P at the 5′-end of the RNA strand was incubated with AMV RT and varying amounts of ligand a.1.1 (Figure 8 A). RNA ligand a.1.1, which inhibits AMV RT polymerization activity, also inhibits AMV RT RNase H activity with an IC_{50} of about 60 nM. We also examined the ability of ligand m.1.1 to inhibit M-MLV RT associated RNase H activity. The RNA ligand m.1.1 did inhibit the cleavage of the RNA strand in the RNA–DNA hybrids by RNase H activity of M-MLV RT (Figure 8B). The IC_{50} of the ligand m.1.1 to M-MLV RT is about 75 nM. It was observed that the cleavage patterns of AMV RT and M-MLV RT RNase H activities are different, but the main cleavage site for both is about 18 base pairs from the 3′-end hydroxyl group of the DNA strand (Kohlstaedt et al., 1992).

DISCUSSION

The repertoire of randomized RNA molecules used in this study was designed to facilitate, but not demand, the formation of pseudoknot structures (Tuerk et al., 1993). It was anticipated that the GCGC fixed sequences would base-pair to each other while the central randomized region would possibly form base pairs with the 3′ or 5′ flanking randomized regions. As shown in our results, secondary structures absent of pseudoknots are also possible. Ultimately, the RNA structures that evolve from the repertoire are determined by the applied intricate selection force. In order to be able to isolate the RNA ligands that are not only tight binders but also inhibitors of their cognate RTs, M-MLV RT was used to synthesize cDNA for the AMV RT selection experiments, and AMV RT was used to generate cDNA for the M-MLV RT and HIV-1 RT (data not shown) selection experiments.

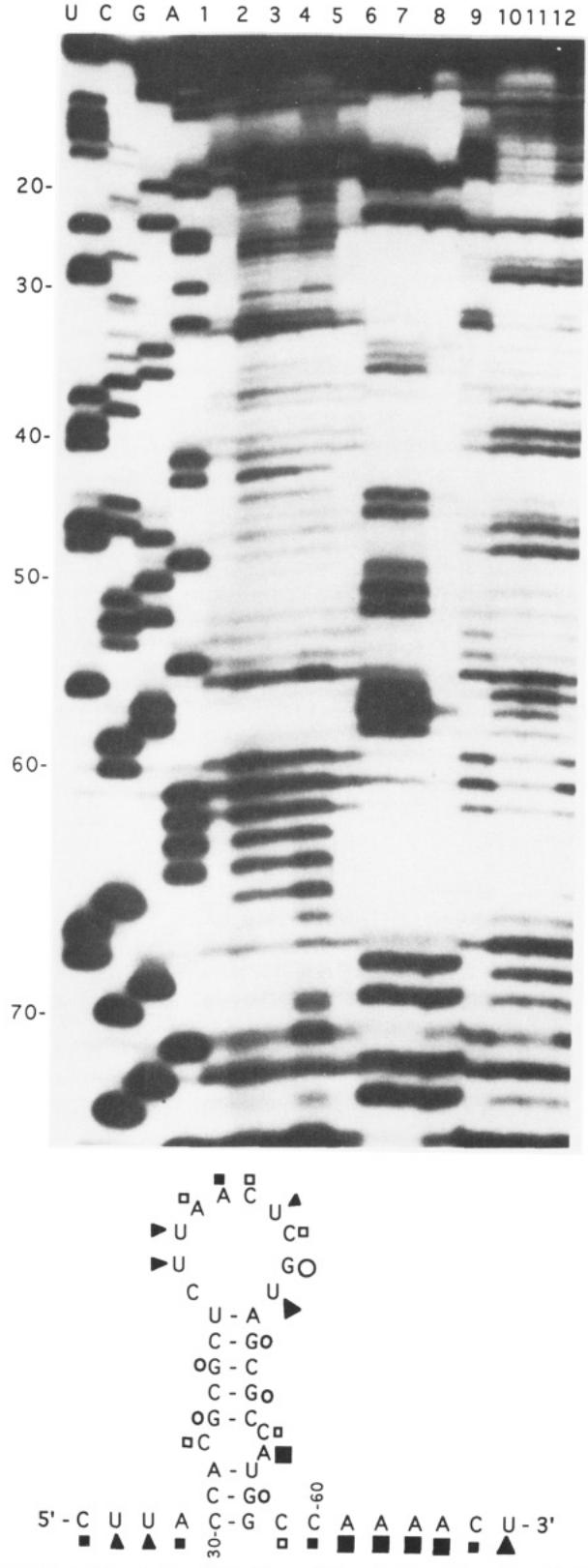

FIGURE 4: Chemical modification and footprinting of ligand m.1.1. (A, top) Autoradiograph of chemical modification and M-MLV RT binding protection of m.1.1. A, G, C, and U, RNA sequencing lanes; lanes 1, 5, and 9, control; lanes 2, 3, and 4, DMS modification, lane 4 in the presence of M-MLV RT; lanes 6, 7, and 8, kethoxal modification, lane 8 in the presence of M-MLV RT; lanes 10, 11, and 12, CMCT modification, lane 12 in the presence of M-MLV RT. Lanes 2, 6, and 10, the modification reactions were carried out immediately, while others were kept on ice for 15 min then carried out modification. The numbers indicate the nucleotide position in RNA ligand m.1.1. (B, bottom) Results of chemical modification. The size of each symbol represents the extent of modification. Squares, DMS modification; circle, KE modification; triangle, CMCT modification. An open symbol means protection of modification in the presence of protein; a filled symbol means modification in the presence of protein.

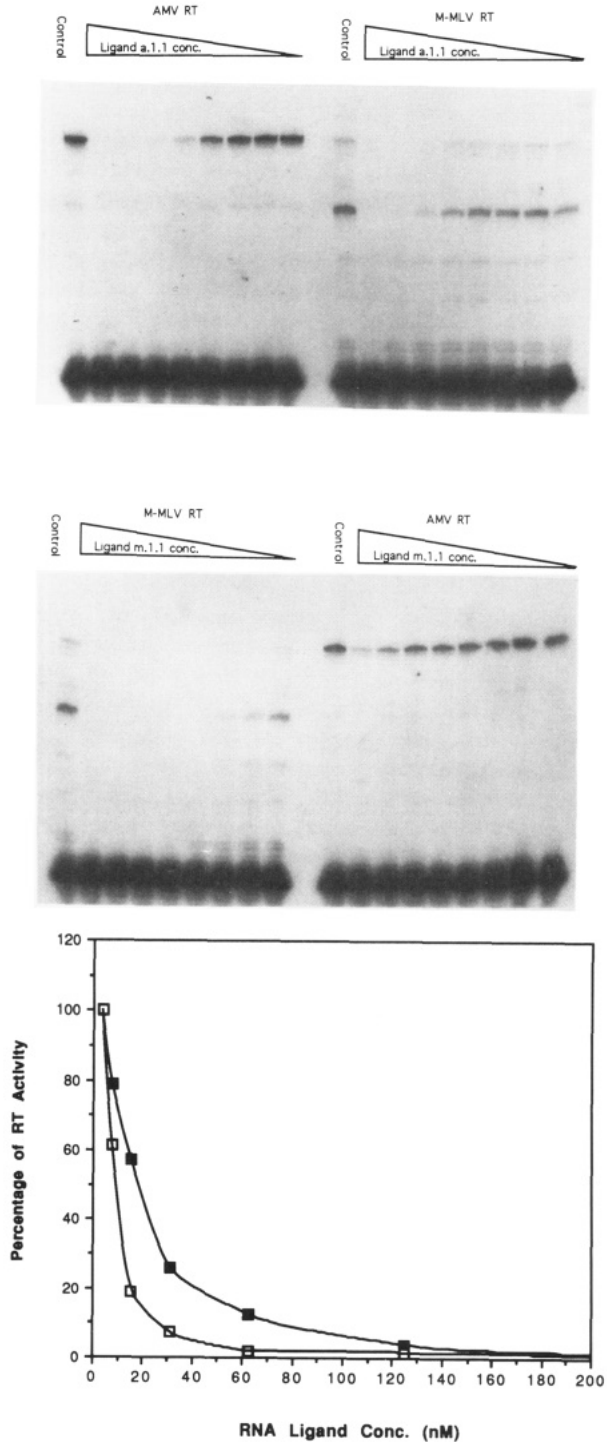

FIGURE 5: Inhibition of RT polymerization activities by selected RNA ligands. Incubation of 3.2 nM reverse transcriptase and 10 nM template/primer complex which is labeled at the 5′-end of the primer with varying amounts of selected RNA ligand a.1.1 or m.1.1 at concentrations ranging from 7.8 to 1000 nM in 20 μL of reaction buffer at 37 °C for 10 min. (A, top left) Inhibition of AMV RT by ligand a.1.1. Control lane indicates the absence of selected ligands. (B, top right) Inhibition of M-MLV RT by ligand a.1.1. (C, middle left) Inhibition of M-MLV RT by ligand m.1.1. (D, middle right) Inhibition of AMV RT by ligand m.1.1. (E, bottom) Quantification of panels A and C by AmBis: –■–, AMV RT inhibited by ligand a.1.1; –□–, M-MLV RT inhibited by ligand m.1.1.

[We also accomplished another parallel experiment by using AMV RT to reverse transcribe the RNA molecules from AMV RT selection. In this case a single species, which is a tight binder with a nanomolar dissociation constant, was isolated, but it failed to inhibit the target (data not shown).] We observed that point mutations and deletions in the GCGC fixed sequences and deletions in the 12-nucleotide randomized

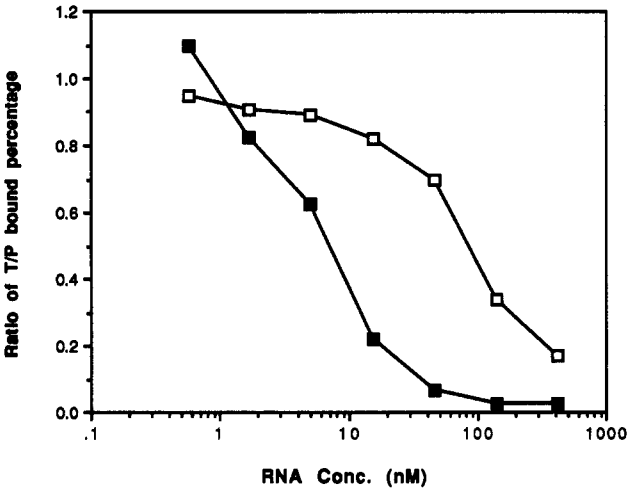

FIGURE 6: Competition of selected RNA ligands with template/primer complex for binding to RTs. -■-, binding competition of ligand a.1.1 with template/primer complex for AMV RT. Incubation of 30 nM ^{32}P-labeled template/primer complex and 30 nM AMV RT with amounts of unlabeled ligand a.1.1 varying from 0.57 up to 417 nM in 60 μL of binding buffer at 37 °C for 5 min. -□-, binding competition of ligand m.1.1 with template/primer complex for M-MLV RT. Incubation of 90 nM ^{32}P-labeled template/primer complex and 90 nM M-MLV RT with amounts of unlabeled ligand m.1.1 varying from 0.57 up to 417 nM in 60 μL of binding buffer at 37 °C for 5 min.

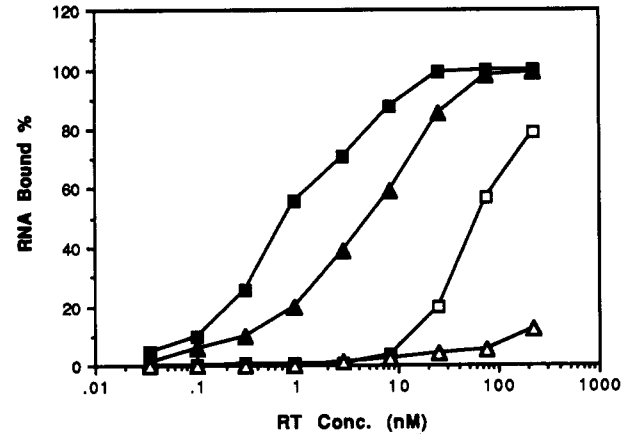

FIGURE 7: Binding affinities of RNA ligands for the cognate and noncognate RTs. The binding reactions were as indicated in the Experimental Procedures section. RNA concentration was 7 × 10^{-11} M, and RT concentration was from 7 × 10^{-11} to 2 × 10^{-7}M. -■-, ligand a.1.1 bound to AMV RT; -□-, ligand a.1.1 bound to M-MLV RT; -▲-, ligand m.1.1 bound to M-MLV RT; -△-, ligand m.1.1 bound to AMV RT.

region were introduced during the selection procedure. These mutations were most likely caused by the infidelities of the polymerases used in the amplification procedures. Reverse transcriptases (Bebenek & Kunkel, 1990; Takeuchi et al., 1988; Roberts et al., 1988) and Taq DNA polymerase (Tindall & Kunkel, 1988; Ennis et al., 1990; Eckert & Kunkel, 1991; Chen et al., 1991) have low fidelities. Interestingly, RNA molecules with mutations, which are assumed to be rare in the population, were preferentially selected.

RNA ligands isolated by AMV RT can be classified into three groups on the basis of their structural similarities: a dual hairpin structure with the highest affinity, pseudoknots, and a stem-loop with internal bulge structures (Table 3 and Figure 1). No obvious consensus sequences have been observed among the three groups. The M-MLV RT selected RNA ligands are classified into two groups. The first group forms a stem-loop structure with an internal bulge, and the second group has the potential to form pseudoknots. A consensus sequence, CCCRRYGAA, was found in the 5′ variable region, and AUACCN$_{2-4}$GUGGC (N can be any of the four nucleotides) was found in the central randomized region of the putative pseudoknots (Table 4). However, no sequence similarities have been observed between those structure groups of each RT selection experiment. We speculated on what might have caused the divergence of the RNA ligands selected by these two enzymes (note that the cDNA synthesis steps required specificity). The crystal structure of HIV-1 RT shows that only one template/primer binding site serves both polymerization and RNase H activities (Kohlstaedt et al., 1992). One possibility might be that some ligands occupy different positions in the active site of the target that are partially overlapped, but distinctive. Another possibility might be that RT may have sites accessible to nucleic acid binding other than the active site.

A comparison of the RNA ligands did not reveal a common conserved sequence selected by AMV, M-MLV, and HIV-1 RT (Tuerk et al., 1993). However, significant secondary structure similarities exist, since putative pseudoknot structures were isolated by all three RT selections. Phylogenetic comparisons of RTs indicate that there are eight conserved amino acid sequence regions spread over the polymerization domain, and five conserved regions in the RNase H domain (Jacobo-Molina & Arnold, 1991; Johnson et al., 1986; Doolittle et al., 1989). The globular three-dimensional structures of RT might be similar, but the detailed topology of the nucleic acid binding sites of the target RT might be different, leading to the differences among the RNA sequences obtained with different targets.

It is reasonable to expect that binding of the selected RNA ligands to RT is similar to that of template/primer complex at the active site in the polymerization domain. The results indicate that this appears to be the case (Figures 5 and 6). RNA ligand a.1.1 inhibits AMV RT efficiently but also somewhat inhibits M-MLV RT activity (IC_{50} equal to 120 nM) (Figure 5B). This result was unexpected because M-MLV RT was used to synthesize cDNA at each cycle of AMV RT selection. If an RNA ligand blocks M-MLV RT activity, it should be eliminated from the pool. The cDNA synthesis for the AMV RT selection was carried out at 45 °C with M-MLV RT; perhaps the RNA structures at that temperature are different from those at 37 °C, the temperature at which inhibition experiments were performed.

Comparing the dissociation constants of ligands a.1.1 (K_d, 0.5 nM) and m.1.1 (K_d, 6.9 nM) for the cognate targets, one might have expected that the inhibition activity of a.1.1 for AMV RT would be higher than that of m.1.1 for M-MLV RT. The first possibility may be that the activity of monomeric M-MLV RT is more susceptible to inhibition by ligand binding. Second, and most important, is the comparison of the dissociation constants of the minimum domain. The K_d of da.1.1 (13.6 nM) for AMV RT is considerably higher than that of the intact ligand a.1.1 (0.5 nM), whereas the dissociation constants of dm.1.1 (18.5 nM) and m.1.1 (6.9 nM) for M-MLV RT are not significantly different. This suggests that nonspecific interactions may contribute to a considerably higher level for the binding of a.1.1 to AMV RT. The inhibition of ligand to the target enzyme is mainly due to the specific binding of ligand to the active site in the enzyme, and thus the inhibition ability of RNA ligands would be more related to the affinity of the minimum domain than to the affinity of the intact molecules. Finally, the dissociation constant of the template/primer complex for AMV RT (12 nM) is considerably lower than that for M-MLV RT (91

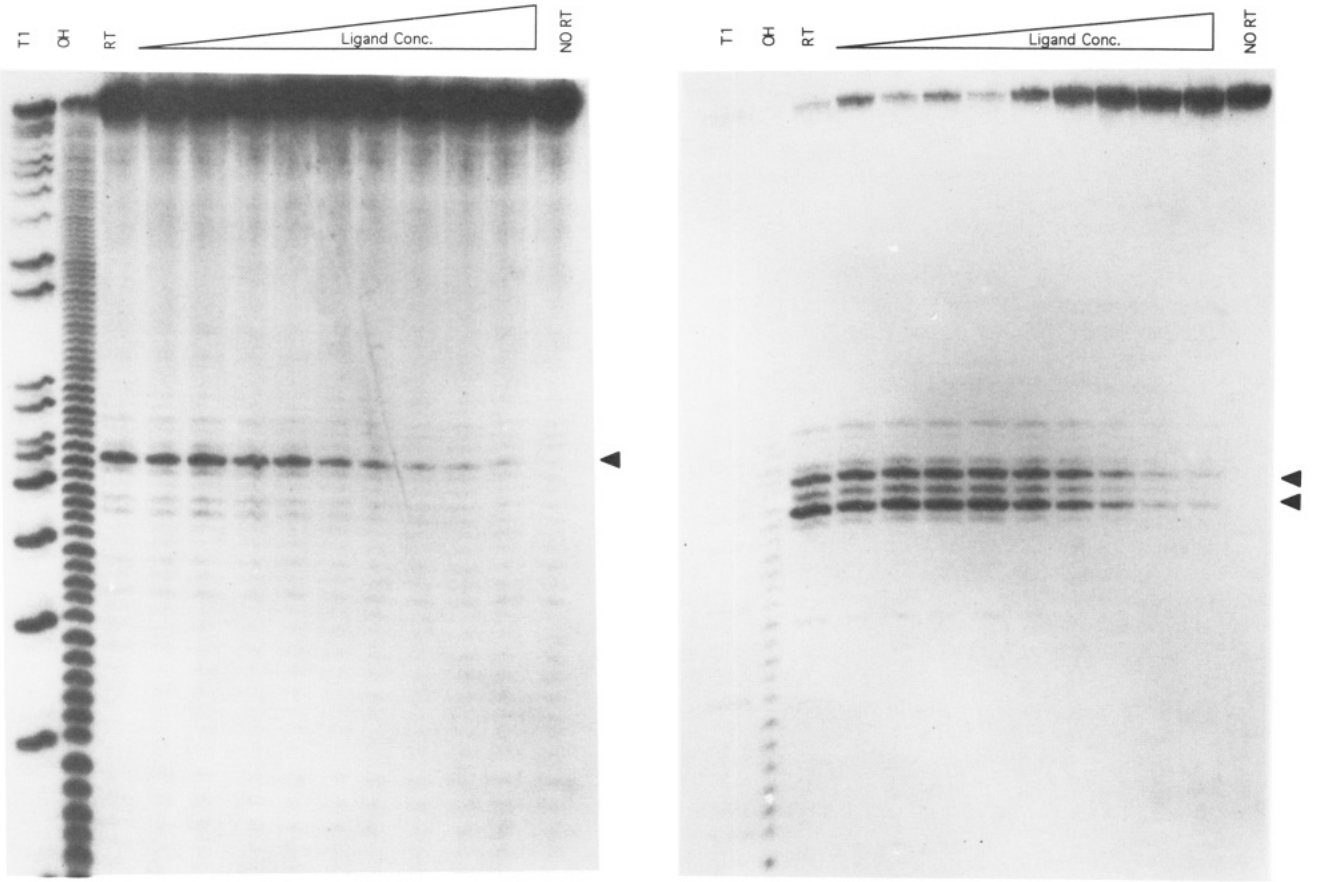

FIGURE 8: Inhibition of RNase H activity by selected RNA ligands: 1.6 nM AMV RT, 3.2 nM M-MLV RT, and 12.5 nM RNA–DNA hybrid labeled at the 5′-end of RNA strand; the concentration of RNA ligand a.1.1 and m.1.1 ranged from 3.9 to 1000 nM. Incubation of each substrate and RT with its cognate ligand was in 20 μL of reaction buffer at 37 °C for 5 min. (A, left) Inhibition of AMV RT RNase H activity by ligand a.1.1. T1, RNase T1 partial hydrolysis; OH, alkaline partial hydrolysis; RT, enzyme only; NO RT, substrate only. Ligand concentration ranged from 3.9 to 1000 nM. (B, right) Inhibition of M-MLV RT RNase H activity by ligand m.1.1. T1, RNase T1 partial hydrolysis; OH, alkaline partial hydrolysis; RT, enzyme only; NO RT, substrate only. Ligand concentration ranged from 3.9 to 1000 nM.

nM); therefore, the primer extension by M-MLV RT would be inhibited more easily by ligand m.1.1.

Reverse transcriptases have a polymerization domain and an RNase H domain. There is evidence that the single template/primer complex binding site serves not only for the polymerization activity but also for the RNase H activity of reverse transcriptase (Krug & Berger, 1991). The distance between the two functional domains is about 16–18 base pairs of A-form helix (Kohlstaedt et al., 1992). Our results indicate that the selected RNA ligand can inhibit the RNA strand hydrolysis in RNA–DNA hybrids by the RNase H activity of the cognate reverse transcriptase (Figure 8). The CI_{50} of ligand a.1.1 to AMV RT at 1.6 nM is about 60 nM, and the CI_{50} of ligand m.1.1 to M-MLV RT at 3.2 nM is approximately 80 nM. The binding of the high-affinity ligand to the nucleic acid binding site on RT probably blocks the binding of the template/primer complex, thereby inhibiting both the polymerization and the RNase H activities. However, we do not yet know whether the selected ligands directly interact with the RNase H domain of RT.

We also compared the binding affinities of the selected inhibitory ligands for the cognate and noncognate targets (Figure 7). The binding affinity of ligand m.1.1 for the noncognate AMV RT is about 3 orders of magnitude lower than that for ligand a.1.1 to AMV RT, while ligand a.1.1 binds to the noncognate M-MLV RT over 80-fold less tightly than m.1.1 binds to M-MLV RT (Figure 7). This indicates that selected ligands can discriminate between two targets within a homologous family.

In summary, high-affinity RNA ligands were isolated by selections with two target reverse transcriptases. Many of the selected RNA molecules have the potential to form pseudoknots. The selected RNA ligands function as inhibitors of the RNA-dependent DNA polymerization activities and RNase H activities of the cognate reverse transcriptases. These RNA ligands will be useful for reverse transcriptase structure probing. The phylogenetic comparison of the RNA shapes selected by closely related reverse transcriptases may provide evolutionary information about their nucleic acid binding sites. The selected RNA inhibitors may also eventually be useful for anti-retroviral therapy.

ACKNOWLEDGMENT

We would like to thank Dr. Steve Ringquist and Dr. Britta Singer for careful reading and scientific suggestions. We thank Dr. Dan Nieuwlandt, Dr. Kevin Morris, Dr. Judy Ruckman, and Dr. Kirk Jensen for helpful discussion. We also thank the W. M. Keck Foundation for their generous support of RNA science on the Boulder Compus.

REFERENCES

Baltimore, D. (1970) *Nature 226*, 209–211.

Barta, A., Steiner, G., Noller, H. F., & Kuechler, E. (1984) *Proc. Natl. Acad. Sci. U.S.A. 81*, 3607–3611.

Bartel, D. P., Zapp, M. L., Green, M. R., & Szostak, J. W. (1991) *Cell 67*, 529–536.

Bebenek, K., & Kunkel, T. A. (1990) *Proc. Natl. Acad. Sci. U.S.A. 87*, 4946–4950.

Bishop, J. M. (1978) *Annu. Rev. Biochem. 47*, 35–88.

Bock, L. C., Griffin, L. C., Latham, J. A., Vermaas, E. H., & Toole, J. J. (1992) *Nature 355*, 564–566.

Chen, J., Sahota, P. J., & Tischfield, J. A. (1991) *Mutat. Res. 249*, 169–176.
Connell, G. J., Illangesekare, M., & Yarus, M. (1993) *Biochemistry 32*, 5497–5502.
Corey, J., Lowary, P. T., & Uhlenbeck, O. C. (1983) *Nucleic Acids Res. 19*, 2601–2615.
Doolittle, R. F., Feng, D.-F., Johnson, M. S., & McClure, M. A. (1989) *Q. Rev. Biol. 64*, 1–27.
Eckert, K. A., & Kunkel, T. A. (1991) *PCR Methods Appl. 1*, 17–24.
Ellington, A., & Szostak, J. (1990) *Nature 346*, 818–822.
Ellington, A., & Szostak, J. (1992) *Nature 355*, 818–822.
Ennis, P. D., Zemmour, J., Salter, R. D., & Parham, P. (1990) *Proc. Natl. Acad. Sci. U.S.A. 87*, 2833–2837.
Furfine, E. S., & Reardon, J. E. (1991) *J. Biol. Chem. 260*, 406–412.
Garret, M., Romby, P., Giege, R., & Litvak, S. (1985) *Nucleic Acids Res. 12*, 2259–2271.
Goff, S. P. (1990) *J. Acquired Immune Defic. Syndr. 3*, 817–831.
Gold, L., Tuerk, C., Allen, P., Binkley, J., Brown, D., Green, L., MacDougal, S., Shneider, D., Tasset, D., & Eddy, S. R. (1993) *The RNA World. RNA: The Shape of Things to Come*, Cold Spring Harbor Laboratory Press, Cold Spring Harbor, NY.
Jacobo-Molina, A., & Arnold, E. (1991) *Biochemistry 30*, 6351–6361.
Jaeger, J. A., Turner, D. H., & Zuker, M. (1989) *Proc. Natl. Acad. Sci. U.S.A. 86*, 7706–7710.
Jellinek, D., Lynott, C. K., Rifkin, D. B., & Janjic, N. (1993) *Proc. Natl. Acad. Sci. U.S.A. 90*, 11227–11231.
Jenison, R. D., Gill, S. C., Pardi, A., & Polisky, B. (1994) *Science 263*, 1425–1429.
Johnson, M. S., McClure, M. A., Feng, D., Gray, J., & Doolittle, R. F. (1986) *Proc. Natl. Acad. Sci. U.S.A. 83*, 7648–7652.
Johnson, M. S., McClure, M. A., Feng, D., Gray, J., & Doolittle, R. F. (1988) *Proc. Natl. Acad. Sci. U.S.A. 85*, 2469–2473.
Klotz, I. M. (1985) *Q. Rev. Biophys. 18*, 227–259.
Kohlstaedt, L. A., Wang, J., Friedman, J. M., Rice, P. A., & Steitz, T. A. (1992) *Science 256*, 1783–1790.
Krug, M. S., & Berger, S. L. (1991) *Biochemistry 30*, 10614–10623.
Kubik, M. F., Shneider, D., Marlar, R. A., & Tasset, D. (1993) *J. Biol. Chem.* (submitted).
Mizrahi, M. (1989) *Biochemistry 28*, 9088–9094.
Oyama, F., Kikuchi, R. J., & Uchida, T. (1989) *J. Biol. Chem. 264*, 18808–18817.
Roberts, J. D., Bebenek, K., & Kunkel, T. A. (1988) *Science 242*, 1171–1173.
Sassanfar, M., & Szostak, J. W. (1993) *Nature 364*, 550–553.
Schneider, D., Tuerk, C., & Gold, L. (1992) *J. Mol. Biol. 228*, 862–869.
Shelness, G. S., & Williams, D. L. (1985) *J. Biol. Chem. 260*, 8637–8646.
Stern, S., Moazed, D., & Noller, H. F. (1988) *Methods Enzymol. 164*, 481–489.
Takeuchi, Y., Nagumo, H., & Hoshino, H. (1988) *J. Virol. 62*, 3900–3902.
Temin, H. M., & Mizutani, S. M. (1970) *Nature 226*, 1211–213.
Tindall, K. R., & Kunkel, T. A. (1988) *Biochemistry 27*, 6008–6013.
Tuerk, C., & Gold, L. (1990) *Science 249*, 505–510.
Tuerk, C., Eddy, S., Parma, D., & Gold, L. (1990) *J. Mol. Biol. 213*, 749–761.
Tuerk, C., MacDougal, S., & Gold, L. (1992) *Proc. Natl. Acad. Sci. U.S.A. 89*, 6988–6992.
Tuerk, C., MacDougal, S., & Gold, L. (1993) in *Polymerase Chain Reaction* (Ferre, F., Mullis, K., Gibbs, R., & Ross, A., Eds.) Birkhauser, New York (in press).
Vaishnav, Y. N., & Wong-Staal, F. (1991) *Annu. Rev. Biochem. 60*, 577–630.
Varmus, H. (1987) *Sci. Am. 3*, 56–64.
Varmus, H. (1988) *Science 240*, 1427–1437.
Varmus, H., & Swanstrom, R. (1984) In *RNA Tumor Viruses* (Weiss, R., Teich, N., Varmus, H., & Coffin, J., Eds.) 2nd ed., pp 369–512, Cold Spring Harbor Laboratory Press, Cold Spring Harbor, NY.
Weiss, R. A., Teich, N., Varmus, H., & Coffin, J. (1982) *Molecular Biology of Tumor Viruses: RNA Tumor Viruses*, Vol. 1, Cold Spring Harbor Laboratory Press, Cold Spring Harbor, NY.
Weiss, R. A., Teich, N., Varmus, H., & Coffin, J. (1985) *Molecular Biology of Tumor Viruses: RNA Tumor Viruses*, Vol. 2, Cold Spring Harbor Laboratory Press, Cold Spring Harbor, NY.
Zuker, M. (1989) *Science 244*, 48–52.